Prelimnary Laboratory Ivestigation Of Cold Wall Anode Materials

Author(s): L. H. Cadoff, I. K. Lloyd, and B. R. Rossing

Session Name: Plasma Properties and Materials

SEAM: 19 (1981)

SEAM EDX URL: https://edx.netl.doe.gov/dataset/seam-19

EDX Paper ID: 907

PRELIMINARY LABORATORY INVESTIGATION OF COLD WALL ANODE MATERIALS*

L. H. Cadoff, I. K. Lloyd, B. R. Rossing
Westinghouse Research and Development Center
Pittsburgh, Pennsylvania

Abstract

The electrochemical corrosion resistance and arc erosion resistance of potential stainless steel and superalloy cold wall electrode materials were evaluated. The results of these studies indicate that cold wall anode degradation is due to the combined and synergistic effects of arc erosion and electrochemical corrosion. High thermal conductivity, the formation of a protective scale and the non-depletion of scale forming constituents under arcing conditions were all found to be desirable anode alloy characteristics.

I. Introduction

The presence of slag/seed layers in coal fired MHD channels can both be detrimental to electrode life and, at the same time, disruptive to current transfer processes.

Recent generator and laboratory experiments indicate that the two major material degradation processes in slag coated channels are erosion by arcing and electrochemical corrosion. Under cold wall operating conditions it is proposed that both reactions can simultaneously contribute to anode loss. This is schematically illustrated in Figure 1 which shows an arc column impinging on a slag coated metal anode and its protective oxide scale. Near the center of the arc column, the slag, the alloy scale and to a lesser extent, the alloy itself is vaporized while in the cooler regions radially outward from the column, designated by L , melting reactions occur. Because of voltage gradients between the plasma and the anode, anions such as O^{-2} and SO_4^{-2} in both the vapor and liquid phases are electrochemically driven towards the anode where they can be discharged by reactions such as:

$$\text{(a)} \quad O^{-2} \rightarrow 1/2\ O_2 + 2e$$

and

$$\text{(b)} \quad SO_4^{-2} \rightarrow SO_3 + 1/2\ O_2 + 2e$$

The presence of these oxidizing, sulfurous atmospheres gives rise at elevated temperatures to accelerated (electro) chemical degradation of alloys often referred to as hot corrosion. Anode arc erosion losses comprise the vaporization/melting of oxide scales and/or alloys as well as the physical spalling of the protective scales due to mechanical and thermal stresses generated by the impinging arc. On the basis of this study, it is clear that anode alloy selection criteria should be based on its being refractory and on its having a refractory protective scale. In addition, the scale must have: high thermal and electrical conductivity, high thermal shock resistance, and high resistance to being fluxed by molten slag/seed mixtures. In this paper, we will report on our recent progress towards developing laboratory scale tests to study both electrochemical corrosion and arc erosion and to understand the reaction mechanisms as they effect a lifetime and performance of potential cold wall MHD anode materials.

Testing

The metals under study in this initial stage of evaluation are commercially available stainless steels and superalloys whose compositions are based upon the Fe-Cr, Ni-Cr, Co-Fe-Cr and Fe-Ni-Cr systems. In addition, tests have been conducted on several pure metals. The results of these tests will form the basis for future development of alloys with compositions and/or microstructures tailored to be more resistant to the MHD environment.

The corrodents used in both the laboratory electrochemical corrosion and the anode arc tests are potassium sulfates. These compounds were selected because generator test results[1,2] strongly indicate that chemical reactions with sulfur containing deposits are a major if not the primary, contributor to anode material loss. While it is the intent of this program to assess material degradation over the entire range of electrode surface temperatures, i.e., from a few hundred degrees Celsius to well over 1000°C; studies, to date, have been conducted in the 573-873K range using $KHSO_4$ (potassium bisulfate) or $K_2S_2O_7$ (potassium pyrosulfate) as the sulfate corrodent/electrolyte. It should be noted that $KHSO_4$ decomposes at approximately 633K, losing water to form $K_2S_2O_7$.

The arc impingement screening test shown in Figure 2 has been designed to simulate the thermal, chemical and electrodynamic environment at cold (<1200K) anode surfaces. In this test, a 2.5 cm. diameter stainless steel test button, clad with the alloy material to be tested, is rotated at 1 rpm. The arc is generated by a plasma needle arc welding unit and is maintained at a constant 5.5 amps over the 1 hour test duration. Voltage drops are approximately 30-35 volts. Constant surface temperatures in the range 250°-600°C are readily maintained by air cooling the back face of the test button. The corrodent which is normally a potassium-sulfur salt is periodically dusted on the sample surface. Corrosion reactions and losses are monitored by chemical analyses, macro- and micro-examination and weight changes.

The anode electrochemical corrosion test is shown schematically in Figure 3. The anode alloy was cleaned, weighed and immersed in the chosen electrolyte along with a platinum cathode. A platinum reference electrode is also inserted to measure anode-cathode, anode-reference and cathode-reference voltages. These voltages are monitored using a digital multimeter and a six channel chart recorder. Temperatures are measured with a thermocouple inserted into the electrolyte. A control sample of the anode alloy was also inserted into

*This work was supported by the U.S. Department of Energy under contact number DE-AC-01-79-ET-15529

the electrolyte to compare reactions and weight changes with and without current. Current at a current density of 0.25-2.00 amp/cm^2 was passed for a measured period, usually 15-150 minutes. Finally, the anode is weighed after cleaning, followed by post-test microscopic and micro-chemical analysis. The loss of material was reported in terms of weight change per coulomb of current passed.

Experimental Results

Electrochemical Tests

The results of electrochemical and anode arc impingement tests are summarized in Table 1. Material loss rates[2] on platinum and four commerical alloys in AVCO's Mark VII generator under high sulfur, coal fired conditions are also shown in Table 1. A comparison of electrochemical test results at 573K and 773K reveals a difference in relative performance of alloys and alloy classes. At 573K the alloys of high iron content are much more resistant to corrosion by molten $KHSO_4$ than alloys containing nickel, cobalt or chromium. In fact, it can be seen from Table 1 that corrosion rates increase with increasing nickel contents in Fe-Ni-Cr alloys. On the other hand, at 773K, the Fe-Ni-Cr alloys (SS 304, SS 310, Incolloy 800 and SS 330) and alloys of high chromium content (SS 446, Haynes 150 and IN-671) are most resistant to corrosion by molten $K_2S_2O_7$.

These results can be understood on the basis of the reaction products formed between the molten sulfates and the alloys. These reaction products could include sulfates, sulfides or oxides which could either dissolve into the melt or grow as a scale on the metal surface. The scales could form as a protective barrier against further reaction between metal and sulfate. The scale morphologies and chemistries could be both variable and complex. The scales formed during the electrochemical tests are very thin (<1 μm thick) and metallographic techniques have not been developed, to date, to identify the chemistry or morphology of any scale. However, by comparing the results on pure metals and scale formation reported on similar alloys in the literature a consistent 'picture' can be made of these results. First, at 573K iron based scales, most probably iron oxides, form which passivates the alloy from corrosive melt-metal electrochemical reactions. These thin layers are electronically conducting so that the electro-chemical interface is now established at the passivated layer/sulfate interface. Electro-chemical reactions involving the generation of gas bubbles will occur here. These passivated layers do not appear to form on high nickel, cobalt or chromium containing alloys. This may be because of unfavorable or slow kinetics at these relatively low temperatures. In any case, these alloys are not a protected scale and electrochem-ical reactions occur at the metal/sulfate interface. Bubble formation will also occur here and that could further increase material losses.

At 773K, the formation kinetics of chromium-based scales is favorable. The protective nature of these scales is dramatically illustrated by comparison of the corrosion rates of chromium at 573K and 773K (see Table 1). These same scales appear to form on the high (>18 w/o) chromium containing alloys with two general exceptions. First, those alloys (IN-601 and IN-690) with high Ni/Cr ratio have corrosion rates similar to that of nickel suggesting that these alloys form scales containing relatively non-protective nickel compounds as scales. Secondly, the somewhat higher corrosion rates of 20Cb-3 and EB 26-1 suggest that alloying elements such as copper, columbium or molybdenum could compromise corrosion resistance of these alloys.

The role of scales in determining corrosion behavior was also demonstrated in a series of experiments where temperature was held constant and the current density was varied. Results on three alloys at 685K are shown in Figure 4. Corrosion rates, in μg/coulomb, increase linearly with increasing current density until a critical current density is reached where upon the corrosion rate becomes independent of current density. The critical current density for a number of alloys over the 573 to 733K temperature range is from 0.3 to 0.5 amps/cm^2. Post-test examination of test specimens showed that below the critical current density a scale had formed on the alloy, while above the critical current density no scale had formed. At the higher current densities these alloys obeyed Faradaic behavior, i.e., corrosion losses are proportional to the quantity of current passed. However, the corrosion efficiencies, experimental losses/theoretical losses x 100%, are in the 10-30% range. This suggests that kinetic factors created by these high current densities may be limiting corrosion rates. Such factors could include surface reaction steps or the transport of reaction products away from the metal interface. While scales are effective in reducing corrosion losses at the lowest current densities they are less and less effective as the current density is measured. This may be due to the erosive effects associated with current transport such as, bubble formation, which may cause turbulent electrolyte flow, and microarcs. Both bubble formation and microarcing increase with increasing current density.

Anode Arc Impingement Tests

To evaluate the relative and synergistic effects on material losses in the anode arc test a series of experiments were first conducted with copper samples. These tests involved: a) heating samples only with a torch (thermal-oxidation effect); (b) heating samples with torch in presence of corrodents (thermal-chemical effects); (c) heating samples with torch and arc (thermal-arc effects); and (d) heating samples with torch and arc in presence of corrodents* (thermal-chemical-arc effects).

The results are shown in Figure 5. It is clear from this data that gross thermal effects alone (dashed curves) are not very important in corrosion. In the worst case, thermal corrosion with K_2SO_4 corrodent results in only 0.07 gm loss at 500°C. However, for the same average surface temperature the imposition of an arc increases corrosion nearly 40 fold to 2.65 gms. This arc accelerated corrosion must be due to either the thermal spike giving rise to enhanced reaction rates at the arc spot and/or electro-chemical reactions between the K_2SO_4 and the copper due to current transfer through the electrolytic corrodent. It is not possible to distinguish between these two mechanisms at present although it is suspected that electro-chemical effects are dominant.

*K_2SO_4, K_2CO_3, Western slag powders

Other important effects shown in Figure 5 are that K_2CO_3 and sulfur free slag are relatively non-reactive with copper even in the presence of an arc and the addition of 20 w/o K_2SO_4 to slag increases arc corrosion by an order of magnitude over sulfate free slag indicating a strong dependence of corrosion on sulfate concentration. This result shows that sulfur masks out corrosion effects due to slag alone and suggests that future tests to evaluate arc corrosion resistance be run with potassium sulfates.

The interpretation of anode arc test data on commercial alloys (see Table 1) is more tenuous than the electrochemical corrosion test results. There appears to be a strong influence of electrochemical corrosion on the arc test data. Most of the alloys that have high losses in the arc test are also those that have poor resistance to $K_2S_2O_7$ at 773K, i.e., IN-601, IN-690, tool steel and FeCrAlY. Also, the relatively poor thermal conductivity of Haynes 150 probably is a major factor in the poor performance of this alloy in the arc test. However, it is difficult to explain the relative ranking of the remaining alloys. In addition, the correlation of the results of this test with results on the same alloys in the AVCO generator is not good.

Metallographic samples from five arc tests examined using the scanning electron microscope (SEM) and energy dispersive analysis (EDS) have provided some insight into arc test material degradation. Evidence of reaction and melting were visible under the SEM in the deepest pits where the conditions have been the most intense. Figure 6 shows both a scale formed by reaction with the sulfate and a fine solidification zone. A comparison of arc test specimens with electrodes run in AVCO's Mark VII generator indicate that the thermal conditions in the arc test are generally more severe. There are two reasons for this: first, the very high heat fluxes in MHD electrode walls allow for much more effective dissipation of the heat from the arc and secondly, the arc in the arc test tends to "hang-up" or resist for periods up to 15 seconds at certain spots. This characteristic, which varies in degree from alloy to alloy, produces craters or pits caused by melting and evaporation of metal. In addition, it introduces a test variable that most probably affects the relative ranking of alloys. More detailed monitoring of these tests could factor out this effect.

SEM/EDS analysis on arc samples of Haynes 150, Inconel 671 and 330 stainless steel showed depletion of chromium in these pits. Figure 6 shows a deep pit in Haynes 150. Near the corrosion surface is a relatively porous scale which is rich in chromium compared to the alloy. Next to the scale is a thin layer of alloy which is severely depleted in chromium (it contains less than half as much chromium as the alloy). Between the severe depletion layer and the base metal there is another layer which is slightly depleted in chromium. This layer shows a fine solidificaiton structure. Inconel 671 and 330 stainless steel behaved like the Haynes 150. In contrast, Ebrite 26-1 and 406 stainless steel showed no evidence of chromium depletion. In a similar examination of various AVCO Mark VII electrodes areas depleted of chromium associated with chromium rich scales have been observed with Inconel 601 and not with either Ebrite 26-1 and 20Cb-3. Further examination of arc test samples and MHD electrodes is in progress but these initial results suggest a degradation process associated with arcing. The arc associated local high temperatures at the alloy surface cause preferential loss of chromium by chromium-rich scale formation and/or by vaporization of chromium from the alloy. These chromium depleted areas are now susceptible to electrochemical corrosion. Examination on both arc test and electrode samples of Ebrite 26-1 further suggest this alloy is not as prone to chromium depletion and therefore to material degradation. While this interpretation is somewhat tentative the point is that the arc test does produce effects similar to that observed in the MHD generator.

In any comparison of the arc erosion of various materials the thermal properties must also be considered. The temperature rise (T_r) of the electrode surface at time (t) after a sudden heat flux (q) is given[3] by

$$T_r = 1.13q\ [t/kc\rho]^{1/2}$$

where k is the thermal conductivity, c the specific heat and p the density of the electrode material. The important quantity is $(kc\rho)^{-1/2}$; on this basis one would expect erosion losses to increase with $(kc\rho)^{-1/2}$. The relative values of $(kc\rho)^{-1/2}$ normalized to Ebrite 26-1 for the alloys tested in the Mark VII are Ebrite 26-1 1.00, 20Cb-3 1.05, SS 330 1.06 and IN-601 1.10. This suggests, that EB 26-1 has the lowest erosion losses because it runs coolest and IN-601 has the highest erosion losses because it runs the hottest. This also suggests that attention to electrode design, from the standpoint of minimizing local temperature rise, and to alloy thermal properties may be a powerful means to reducing erosion losses and extending electrode life.

Conclusions

Although detailed analysis of the reaction mechanisms of potential metal electrode materials with potassium sulfur environments is still in the early stages of investigation, our laboratory experiments show:

1) Low temperature (573K) electrochemical corrosion reactions in $KHSO_4$ melts are related to the absence of protective scale formation. In general iron rich superalloys are the most corrosion resistant while nickel rich superalloys are the least corrosion resistant.

2) At intermediate temperatures (773K) superalloys electrochemically corroded in $KHSO_4$-$K_2S_2O_7$ melts tend to develop chromium rich protective scales. The corrosion rate generally decreases as Cr/Ni ratio increases in a nickel alloy.

3) Arc corrosion is very sensitive to the sulfur content of the corrodent. Superalloys containing chromium which have low thermal diffusivities tend to superheat locally. The high local temperatures then contribute to chromium depletion leaving the area vulnerable to rapid corrosion attack. Conversely, alloys with high thermal conductivities and metal electrodes designed for rapid heat fluxes exhibit relatively low corrosion rates. These alloys and

designs tend to dissipate thermal spikes minimizing chromium depletion.

4) The corrosion of cold metal electrodes is a complex process. It is related to both electrochemical and arc attack. Continued laboratory investigations combined with detailed comparisons with the channel data will in the future permit a better understanding of the corrosion mechanisms. This understanding will be used to optimize alloy selection criteria.

Acknowledgments

The authors would like to thank R. J. Veenis and S. R. Westover for their valuable contributions during these investigations.

References

1. Heywood J. B. and Womack G. J., Open Cycle MHD Power Generation, Pergamon Press, London (1969).

2. V. J. Hruby et al., "Electrode Development at AVCO Everett Research Laboratory Inc.", 7th Int. Conf. on MHD Power Generation, Cambridge, MA, June 1980.

3. H. S. Carslaw and J. C. Jaeger, Conduction of Heat in Solids, Claredon Press, Oxford, (1962).

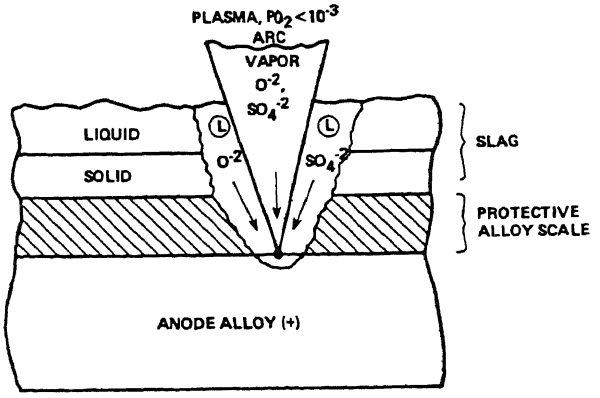

Figure 1. Schematic of Arc Impingement on Slag Covered Alloy Anode

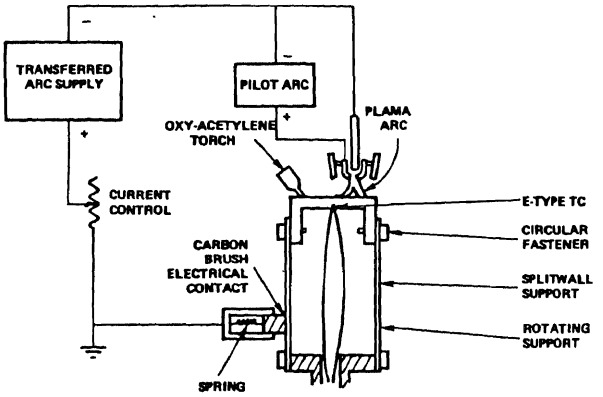

Figure 2. Schematic of Anode-Arc Corrosion Test

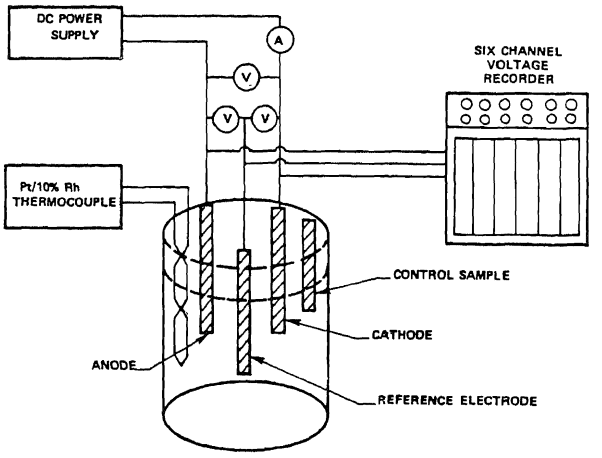

Figure 3. Schematic of Electrochemical Corrosion Test

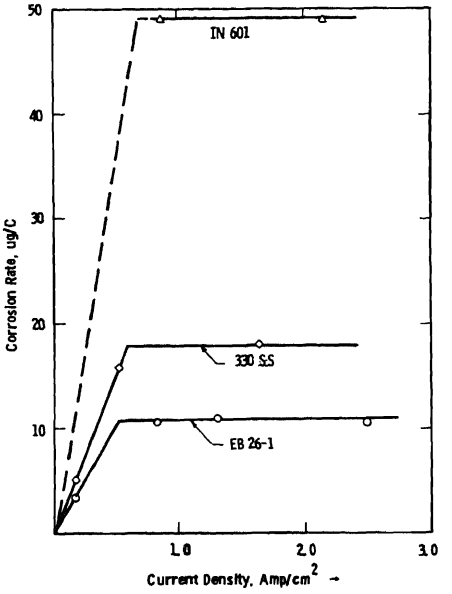

Figure 4. Corrosion rates of IN-601, 330 SS, and EB 26-1 as a function of current density at 658K

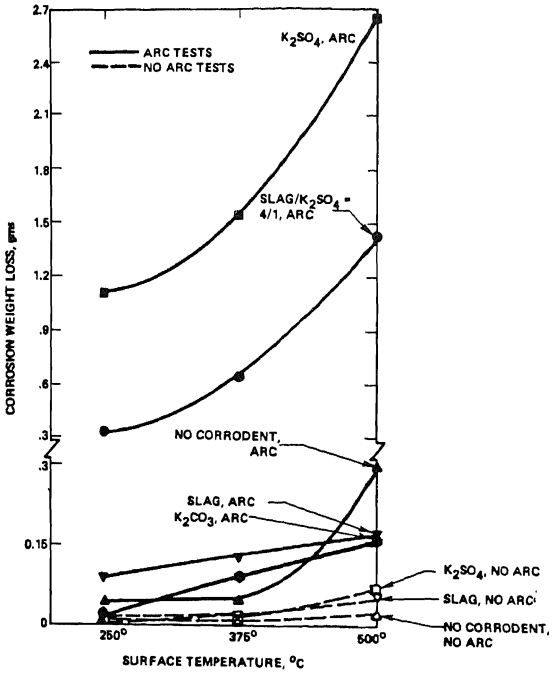

Figure 5. The Effect of Arc, Corrodents and Surface Temperature on Corrosion of Copper

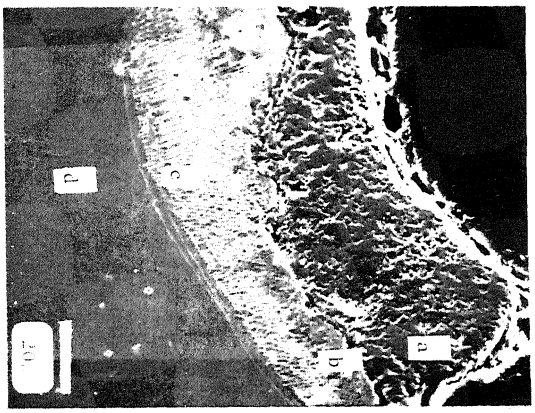

Figure 6. SEM of an Arc Pit in a H150 Laboratory Arc Specimen: a) scale b) severe chromium depletion layer, c) mild chromium depletion and rapid solidification zone, d) base metal.

TABLE I

EROSION/CORROSION RATES OF COMMERCIAL ALLOYS AND PURE METALS IN VARIOUS MHD TESTS

	Major Components w/o					EROSION/CORROSION RATES μg/C			
						ELECTROCHEMICAL ~.25 A/cm^2		ARC**	AVCO[2]
	Fe	Ni	Cr	Al	Other	573K*	773K**	773K	773K
Platinum					100 Pt	0.79	0.43	0.55	0.5
Tool Steel A-2	91.5		5.5			1.8	26	16.3	
SS 406	83		13	4		4.7	18	8.78	
FeCrAlY	80		15	5		5.5	28	12.6	
SS 446	725		25			5.6	12	6.72	
EB 26-1	72		26			5.6	18	12.2	2.2
SS 304	70	9	19			8.7	10	8.46	
SS 310	52.5	21	25			42	10	8.37	
IN 800	44	32.5	21	.4		60	10	8.51	
20Cb3	43	35	20.5			54	18	20.9	3.9
SS 330	43	35	19.5			65	10	4.32	7.0
IN 601	14	60.5	23	1.35		105	38	16.9	7.2
IN 690	10	60	30			92	48	13.4	
IN 671		52	48			128	9.3	8.18	
Haynes 150	21		28		50 Co	35	13	14.8	
Nickel		100				102	48		
Cobalt					100 Co	22	150		
Iron	100					1.6	26		
Chromium			100			132	11		
Copper					100 Cu	654	3900		150

*$KHSO_4$

**90 $K_2S_2O_7$-10 $KHSO_4$